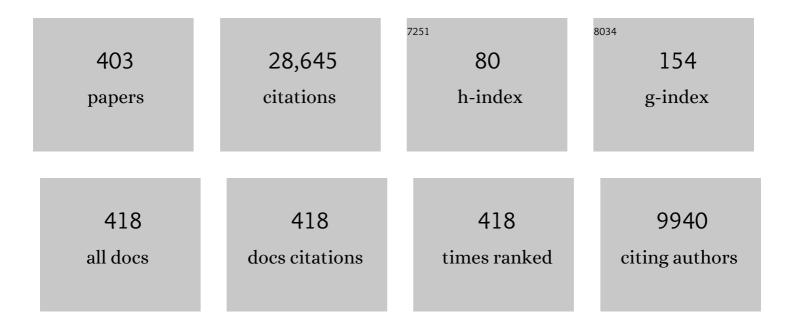
List of Publications by Year in descending order

Source: https://exaly.com/author-pdf/7502252/publications.pdf Version: 2024-02-01



ΔΝΠΩΕΙ ΔΤΩΕΝΟ

#	Article	lF	CITATIONS
1	A Mg alloy with no hydrogen evolution during dissolution. Journal of Magnesium and Alloys, 2023, 11, 2084-2095.	5.5	13
2	Enhanced initial biodegradation resistance of the biomedical Mg-Cu alloy by surface nanomodification. Journal of Magnesium and Alloys, 2023, 11, 2776-2788.	5.5	11
3	Active corrosion protection of phosphate loaded PEO/LDHs composite coatings: SIET study. Journal of Magnesium and Alloys, 2022, 10, 1351-1357.	5.5	28
4	Corrosion of Mg Alloys. , 2022, , 46-74.		3
5	The influence of Ga alloying on Mg-Al-Zn alloys as anode material for Mg-air primary batteries. Electrochimica Acta, 2022, 401, 139372.	2.6	19
6	Influence of heat treatment on the discharge performance of Mg-Al and Mg-Zn alloys as anodes for the Mg-air battery. Chemical Engineering Journal, 2022, 433, 133797.	6.6	25
7	The discharge performance of an as-extruded Mg-Zn-La-Ce anode for the primary Mg-air battery. Electrochimica Acta, 2022, 404, 139763.	2.6	18
8	Effect of scratch on corrosion resistance of calciumphosphate conversioncoated AZ80 magnesium alloy. Transactions of Nonferrous Metals Society of China, 2022, 32, 147-161.	1.7	6
9	Influence of Si, Cu, B, and Trace Alloying Elements on the Conductivity of the Al-Si-Cu Alloy. Materials, 2022, 15, 426.	1.3	1
10	The influence of the protein bovine serum albumin (BSA) on the corrosion of Mg, Zn, and Fe in Zahrina's simulated interstitial fluid. Corrosion Science, 2022, 199, 110160.	3.0	10
11	Effect of shearing prestrain on the hydrogen embrittlement of 1180ÂMPa grade martensitic advanced high-strength steel. Corrosion Science, 2022, 199, 110170.	3.0	10
12	Influence of crystallographic orientation and Al alloying on the corrosion behaviour of extruded α-Mg/LPSO two-phase Mg-Zn-Y alloys with multimodal microstructure. Corrosion Science, 2022, 200, 110237.	3.0	27
13	Design, mechanical and degradation requirements of biodegradable metal mesh for pelvic floor reconstruction. Biomaterials Science, 2022, 10, 3371-3392.	2.6	6
14	Deep Cryogenic Treatment Characteristics of a Deformation-Processed Cu-Ni-Co-Si Alloy. Materials, 2022, 15, 3051.	1.3	1
15	Effect of cold deformation on the hydrogen permeation in a dual-phase advanced high-strength steel. Electrochimica Acta, 2022, 424, 140619.	2.6	5
16	A novel dissolution-precipitation mechanism during liquid phase sintering and its strengthening effects in W-Ni-Fe alloys with low W contents. Materials and Design, 2022, 220, 110841.	3.3	9
17	The influence of phosphorus on the temper embrittlement and hydrogen embrittlement of some dual-phase steels. Materials Science & Engineering A: Structural Materials: Properties, Microstructure and Processing, 2022, 854, 143379.	2.6	5
18	Influence of hydrogen on the S–N fatigue of DP1180 advanced high-strength steel. Corrosion Science, 2022, 205, 110465.	3.0	4

#	Article	IF	CITATIONS
19	Discharge properties and electrochemical behaviors of AZ80-La-Gd magnesium anode for Mg-air battery. Journal of Magnesium and Alloys, 2021, 9, 2113-2121.	5.5	31
20	Surface modification of biomedical Mg-Ca and Mg-Zn-Ca alloys using selective laser melting: Corrosion behaviour, microhardness and biocompatibility. Journal of Magnesium and Alloys, 2021, 9, 2155-2168.	5.5	20
21	Effect of cooling rate on microstructure and mechanical properties of a low-carbon low-alloy steel. Journal of Materials Science, 2021, 56, 3995-4005.	1.7	21
22	Effect of corrosion inhibiting compounds on the corrosion behaviour of pure magnesium and the magnesium alloys EV31A, WE43B and ZE41A. Journal of Magnesium and Alloys, 2021, 9, 432-455.	5.5	21
23	Influence of commercial corrosionâ€inhibiting compounds on the atmospheric corrosion of the magnesium alloys EV31A, WE43B, ZE41A and pure magnesium. Materials and Corrosion - Werkstoffe Und Korrosion, 2021, 72, 672-693.	0.8	7
24	The influence of heat treatment on discharge and electrochemical properties of Mg-Gd-Zn magnesium anode with long period stacking ordered structure for Mg-air battery. Electrochimica Acta, 2021, 367, 137518.	2.6	46
25	Hydrogen-induced delayed fracture of a 1180†MPa martensitic advanced high-strength steel under U-bend loading. Materials Today Communications, 2021, 26, 101887.	0.9	3
26	Morphology, microstructure and tribological properties of anodic films formed on Ti10V2Fe3Al alloy in different electrolytes. Rare Metals, 2021, 40, 1-12.	3.6	4
27	Effects of deformation processes on morphology, microstructure and corrosion resistance of LDHs films on magnesium alloy AZ31. Journal of Materials Science and Technology, 2021, 64, 10-20.	5.6	50
28	Doublely-doped Mg-Al-Ce-V2O74- LDH composite film on magnesium alloy AZ31 for anticorrosion. Journal of Materials Science and Technology, 2021, 64, 66-72.	5.6	79
29	A comprehensive review of the development of magnesium anodes for primary batteries. Journal of Materials Chemistry A, 2021, 9, 12367-12399.	5.2	72
30	Understanding the discharge behavior of an ultra-high-purity Mg anode for Mg–air primary batteries. Journal of Materials Chemistry A, 2021, 9, 21387-21401.	5.2	27
31	In Vitro Corrosion Resistance and Antibacterial Performance of Novel Fe– <i>x</i> Cu Biomedical Alloys Prepared by Selective Laser Melting. Advanced Engineering Materials, 2021, 23, 2001000.	1.6	15
32	Biodegradation behaviour of hydroxyapatite-containing self-sealing micro-arc-oxidation coating on pure Mg. Surface Engineering, 2021, 37, 942-952.	1.1	15
33	Comparison on Tensile Characteristics of Plain C–Mn Steel with Ultrafine Grained Ferrite/Cementite Microstructure and Coarse Grained Ferrite/Pearlite Microstructure. Materials, 2021, 14, 2309.	1.3	6
34	Effect of NaOH concentration on microstructure and corrosion resistance of MAO coating on cast Alâ^'Li alloy. Transactions of Nonferrous Metals Society of China, 2021, 31, 913-924.	1.7	21
35	Corrosion and antibacterial performance of novel selective-laser-melted (SLMed) Ti-xCu biomedical alloys. Journal of Alloys and Compounds, 2021, 864, 158415.	2.8	29
36	The feasibility and limitation of urine as the electrolyte for primary Mg-air batteries. Ionics, 2021, 27, 2733-2737.	1.2	3

#	Article	IF	CITATIONS
37	Hydrogen fracture maps for sheared-edge-controlled hydrogen-delayed fracture of 1180 MPa advanced high-strength steels. Corrosion Science, 2021, 184, 109360.	3.0	18
38	Effect of vanadium and rare earth microalloying on the hydrogen embrittlement susceptibility of a Fe-18Mn-0.6C TWIP steel studied using the linearly increasing stress test. Corrosion Science, 2021, 185, 109440.	3.0	27
39	Study on a Novel Biodegradable and Antibacterial Fe-Based Alloy Prepared by Microwave Sintering. Materials, 2021, 14, 3784.	1.3	11
40	Corrosion and discharge behavior of Mgâ^'xLa alloys (x=0.0â^'0.8) as anode materials. Transactions of Nonferrous Metals Society of China, 2021, 31, 1979-1992.	1.7	14
41	Hydrogen-induced fast fracture in notched 1500 and 1700 MPa class automotive martensitic advanced high-strength steel. Corrosion Science, 2021, 188, 109550.	3.0	21
42	Two distinct roles of Al2Sm and Al11Sm3 phases on the corrosion behavior of the magnesium alloy Mg-5Sm-xAl. Progress in Natural Science: Materials International, 2021, 31, 599-608.	1.8	10
43	Influence of indentation size on the corrosion behaviour of a phosphate conversion coated AZ80 magnesium alloy. Journal of Materials Research and Technology, 2021, 14, 1739-1753.	2.6	14
44	MgAl-V2O7 4- LDHs/(PEI/MXene)10 composite film for magnesium alloy corrosion protection. Journal of Materials Science and Technology, 2021, 91, 28-39.	5.6	38
45	Comparison of the biodegradation of ZK30 subjected to solid solution treating and selective laser melting. Journal of Materials Research and Technology, 2021, 10, 722-729.	2.6	15
46	The high-temperature oxidation resistance properties of magnesium alloys alloyed with Gd and Ca. Journal of Materials Science, 2021, 56, 8745-8761.	1.7	20
47	Anodic hydrogen evolution on Mg. Journal of Magnesium and Alloys, 2021, 9, 2049-2062.	5.5	30
48	Discharge properties of Mg-Sn-Y alloys as anodes for Mg-air batteries. International Journal of Minerals, Metallurgy and Materials, 2021, 28, 1705-1715.	2.4	16
49	Biodegradation, Antibacterial Performance, and Cytocompatibility of a Novel ZK30-Cu-Mn Biomedical Alloy Produced by Selective Laser Melting. International Journal of Bioprinting, 2021, 7, 300.	1.7	3
50	Study on Fe-xGO Composites Prepared by Selective Laser Melting: Microstructure, Hardness, Biodegradation and Cytocompatibility. Jom, 2020, 72, 1163-1174.	0.9	14
51	Effects of external field treatment on the electrochemical behaviors and discharge performance of AZ80 anodes for Mg-air batteries. Journal of Materials Science and Technology, 2020, 38, 47-55.	5.6	60
52	Microstructure, mechanical properties and corrosion behavior of quasicrystal-reinforced Mg-Zn-Y alloy subjected to dual-frequency ultrasonic field. Corrosion Science, 2020, 163, 108289.	3.0	38
53	Corrosion of Mg alloys EV31A, WE43B, and ZE41A in chloride―and sulfateâ€containing solutions saturated with magnesium hydroxide. Materials and Corrosion - Werkstoffe Und Korrosion, 2020, 71, 956-979.	0.8	17
54	Review of Mg alloy corrosion rates. Journal of Magnesium and Alloys, 2020, 8, 989-998.	5.5	212

ANDREJ ATRENS

#	Article	IF	CITATIONS
55	The effects of Ca and Mn on the microstructure, texture and mechanical properties of Mg-4 Zn alloy. Journal of Magnesium and Alloys, 2020, , .	5.5	59
56	Enhanced protective nanoparticle-modified MgAl-LDHs coatings on titanium alloy. Surface and Coatings Technology, 2020, 404, 126449.	2.2	12
57	Effect of Alloying Mn by Selective Laser Melting on the Microstructure and Biodegradation Properties of Pure Mg. Metals, 2020, 10, 1527.	1.0	5
58	Effect of Al on the microstructure, corrosion behavior and mechanical properties of Mg-4Li. Anti-Corrosion Methods and Materials, 2020, 67, 31-37.	0.6	6
59	Influence of graphene oxide (GO) on microstructure and biodegradation of ZK30-xGO composites prepared by selective laser melting. Journal of Magnesium and Alloys, 2020, 8, 952-962.	5.5	28
60	Microstructure modification and corrosion resistance enhancement of die-cast Mg-Al-Re alloy by Sr alloying. Journal of Magnesium and Alloys, 2020, 9, 950-950.	5.5	28
61	Microstructure and Strengthening Model of Cu–Fe In-Situ Composites. Materials, 2020, 13, 3464.	1.3	15
62	What activates the Mg surface—A comparison of Mg dissolution mechanisms. Journal of Materials Science and Technology, 2020, 57, 204-220.	5.6	72
63	Hydrogen embrittlement of an automotive 1700 MPa martensitic advanced high-strength steel. Corrosion Science, 2020, 171, 108726.	3.0	42
64	Influence of trace As content on the microstructure and corrosion behavior of the AZ91 alloy in different metallurgical conditions. Journal of Magnesium and Alloys, 2020, 8, 301-317.	5.5	33
65	Microstructural evolution upon heat treatments and its effect on corrosion in Al-Zn-Mg alloys containing Sc and Zr. Journal of Materials Research and Technology, 2020, 9, 5077-5089.	2.6	29
66	Microstructure and corrosion behavior of Mg-Sc binary alloys in 3.5 wt.% NaCl solution. Corrosion Science, 2020, 174, 108831.	3.0	90
67	Effect of Steels on the Purity of Molten Mg Alloys. Advanced Engineering Materials, 2020, 22, 2000338.	1.6	18
68	The role of longâ€period stacking ordered phase on the discharge and electrochemical behaviors of magnesium anode Mgâ€Znâ€Y for the primary Mgâ€air battery. International Journal of Energy Research, 2020, 44, 8865-8876.	2.2	32
69	Corrosion behavior of a self-sealing coating containing CeO2 particles on pure Mg produced by micro-arc oxidation. Surface and Coatings Technology, 2020, 386, 125456.	2.2	53
70	Effect of microalloyed Ca on the microstructure and corrosion behavior of extruded Mg alloy AZ31. Journal of Alloys and Compounds, 2020, 823, 153844.	2.8	43
71	Superhydrophobic coatings for corrosion protection of magnesium alloys. Journal of Materials Science and Technology, 2020, 52, 100-118.	5.6	164
72	Microstructures and Mechanical Properties of Mg–xAl–1Sn–0.3Mn (x = 1, 3, 5) Alloy Sheets. Acta Metallurgica Sinica (English Letters), 2020, 33, 1217-1225.	1.5	4

#	Article	IF	CITATIONS
73	Effect of plastic strain damage on the hydrogen embrittlement of a dual-phase (DP) and a quenching and partitioning (Q&P) advanced high-strength steel. Materials Science & Engineering A: Structural Materials: Properties, Microstructure and Processing, 2020, 785, 139343.	2.6	20
74	The influence of samarium (Sm) on the discharge and electrochemical behaviors of the magnesium alloy AZ80 as an anode for the Mg-air battery. Electrochimica Acta, 2020, 348, 136315.	2.6	60
75	Effect of the Al–Si eutectic on the microstructure and corrosion behavior of the single-phase Mg alloy Mg–4Li. Journal of Magnesium and Alloys, 2020, 9, 1339-1339.	5.5	26
76	The quasicrystal of Mg–Zn–Y on discharge and electrochemical behaviors as the anode for Mg-air battery. Journal of Power Sources, 2020, 451, 227807.	4.0	95
77	Quantifying the influence of calcium ion concentration on the corrosion of high-purity magnesium, AZ91, WE43 in modified Hanks' solutions. Materials Research Express, 2020, 7, 096501.	0.8	3
78	Enhancement of Corrosion Resistance and Discharge Performance of Mg–5Li–3Al–1Zn Sheet for Mg-air Battery via Rolling. Journal of the Electrochemical Society, 2020, 167, 110529.	1.3	23
79	Corrosion of metallic biomaterials. , 2020, , 469-515.		4
80	Formation and characteristic corrosion behavior of alternately lamellar arranged α and β in as-cast AZ91 Mg alloy. Journal of Alloys and Compounds, 2019, 770, 549-558.	2.8	49
81	Influence of Tempering Temperature on the Microstructure and Mechanical Properties of a Cr–Ni–Moâ€Alloyed Steel for Rock Drill Applications. Steel Research International, 2019, 90, 1900297.	1.0	4
82	Evolution of microstructure and texture for an Al-0.4 Er alloy during accumulative roll bonding. Journal of Alloys and Compounds, 2019, 811, 152005.	2.8	9
83	Influence of Microalloying with Ca and Ce on the Corrosion Behavior of Extruded Mg-3Al-1Zn. Journal of the Electrochemical Society, 2019, 166, C445-C453.	1.3	21
84	Simultaneously improving elastic modulus and damping capacity of extruded Mg-Gd-Y-Zn-Mn alloy via alloying with Si. Journal of Alloys and Compounds, 2019, 810, 151857.	2.8	43
85	Structure and rheology of liquid crystal hydroglass formed in aqueous nanocrystalline cellulose suspensions. Journal of Colloid and Interface Science, 2019, 555, 702-713.	5.0	21
86	Novel β-Ti35Zr28Nb alloy scaffolds manufactured using selective laser melting for bone implant applications. Acta Biomaterialia, 2019, 87, 273-284.	4.1	85
87	Improvement of biodegradable and antibacterial properties by solution treatment and micro-arc oxidation (MAO) of a magnesium alloy with a trace of copper. Corrosion Science, 2019, 156, 125-138.	3.0	64
88	Coupled hydrogen and phosphorous induced initiation of internal cracks in a large 18MnNiMo5 component. Engineering Failure Analysis, 2019, 104, 422-438.	1.8	8
89	Absorbable Mg surgical tack: Proof of concept & in situ fixation strength. Journal of the Mechanical Behavior of Biomedical Materials, 2019, 97, 321-329.	1.5	16
90	Graphene Oxide Reinforced Iron Matrix Composite With Enhanced Biodegradation Rate Prepared by Selective Laser Melting. Advanced Engineering Materials, 2019, 21, 1900314.	1.6	17

#	Article	IF	CITATIONS
91	Review of the atmospheric corrosion of magnesium alloys. Journal of Materials Science and Technology, 2019, 35, 2003-2016.	5.6	129
92	Corrosion resistance of fatty acid and fluoroalkylsilane-modified hydrophobic Mg-Al LDH films on anodized magnesium alloy. Applied Surface Science, 2019, 487, 569-580.	3.1	100
93	Effect of Boron on the Grain Refinement and Mechanical Properties of as-Cast Mg Alloy AM50. Materials, 2019, 12, 1100.	1.3	7
94	Fabrication and characterization of an actively protective Mg-Al LDHs/Al2O3 composite coating on magnesium alloy AZ31. Applied Surface Science, 2019, 487, 558-568.	3.1	59
95	Understanding the corrosion behaviour of the magnesium alloys EV31A, WE43B, and ZE41A. Materials and Corrosion - Werkstoffe Und Korrosion, 2019, 70, 1527-1552.	0.8	33
96	Biodegradation Behavior of Coated As-Extruded Mg–Sr Alloy in Simulated Body Fluid. Acta Metallurgica Sinica (English Letters), 2019, 32, 1195-1206.	1.5	26
97	Effects of Fe concentration on microstructure and corrosion of Mg-6Al-1Zn-xFe alloys for fracturing balls applications. Journal of Materials Science and Technology, 2019, 35, 2086-2098.	5.6	44
98	In-situ grown super- or hydrophobic Mg-Al layered double hydroxides films on the anodized magnesium alloy to improve corrosion properties. Surface and Coatings Technology, 2019, 366, 238-247.	2.2	53
99	Ultra-high cycle fatigue behavior of a novel 1.9â€ <sup>−</sup> GPa grade super-high-strength maraging stainless steel. Materials Science & Engineering A: Structural Materials: Properties, Microstructure and Processing, 2019, 755, 50-56.	2.6	14
100	Smart epoxy coating containing zeolites loaded with Ce on a plasma electrolytic oxidation coating on Mg alloy AZ31 for active corrosion protection. Progress in Organic Coatings, 2019, 132, 144-147.	1.9	39
101	Recent understanding of the oxidation and burning of magnesium alloys. Surface Innovations, 2019, 7, 71-92.	1.4	33
102	Strain hardening behavior of Mg–Y alloys after extrusion process. Journal of Magnesium and Alloys, 2019, 7, 672-680.	5.5	65
103	Effect of Li content on microstructure and mechanical property of Mg−xLi−3(Al−Si) alloys. Transactions of Nonferrous Metals Society of China, 2019, 29, 2506-2513.	1.7	25
104	Strain hardening of as-extruded Mg-xZn (x = 1, 2, 3 and 4 wt%) alloys. Journal of Materials Science and Technology, 2019, 35, 142-150.	5.6	105
105	Corrosion of porous Ti35Zr28Nb in Hanks' solution and 3.5 wt% NaCl. Materials and Corrosion - Werkstoffe Und Korrosion, 2019, 70, 529-536.	0.8	6
106	A Graphene Spin Coatings for Cost-Effective Corrosion Protection for the Magnesium Alloy AZ31. Journal of Nanoscience and Nanotechnology, 2019, 19, 105-111.	0.9	7
107	Improved biodegradation resistance by grain refinement of novel antibacterial ZK30-Cu alloys produced via selective laser melting. Materials Letters, 2019, 237, 253-257.	1.3	57
108	Investigating Mg Biocorrosion In Vitro: Lessons Learned and Recommendations. Jom, 2019, 71, 1406-1413.	0.9	34

#	Article	IF	CITATIONS
109	Generalisation of the oxide reinforcement model for the high oxidation resistance of some Mg alloys micro-alloyed with Be. Corrosion Science, 2019, 147, 357-371.	3.0	30
110	Effect of grain refinement and crystallographic texture produced by friction stir processing on the biodegradation behavior of a Mg-Nd-Zn alloy. Journal of Materials Science and Technology, 2019, 35, 777-783.	5.6	77
111	The Corrosion Behavior of Mg5Y in Nominally Distilled Water. Advanced Engineering Materials, 2018, 20, 1700986.	1.6	9
112	Further study of the hydrogen embrittlement of martensitic advanced high-strength steel in simulated auto service conditions. Corrosion Science, 2018, 135, 120-135.	3.0	42
113	Cu-7Cr-0.1Ag Microcomposites Optimized for High Strength and High Condutivity. Journal of Materials Engineering and Performance, 2018, 27, 933-938.	1.2	6
114	Building towards a standardised approach to biocorrosion studies: a review of factors influencing Mg corrosion in vitro pertinent to in vivo corrosion. Science China Materials, 2018, 61, 475-500.	3.5	50
115	Determination of the equivalent hydrogen fugacity during electrochemical charging of 3.5NiCrMoV steel. Corrosion Science, 2018, 132, 90-106.	3.0	55
116	The role of the microstructure on the influence of hydrogen on some advanced high-strength steels. Materials Science & Engineering A: Structural Materials: Properties, Microstructure and Processing, 2018, 715, 370-378.	2.6	57
117	Improved oxidation resistance of Mg-9Al-1Zn alloy microalloyed with 60 wt ppm Be attributed to the formation of a more protective (Mg,Be)O surface oxide. Corrosion Science, 2018, 132, 272-283.	3.0	31
118	Sealing of anodized magnesium alloy AZ31 with MgAl layered double hydroxides layers. RSC Advances, 2018, 8, 2248-2259.	1.7	109
119	Effect of Micro-Arc Oxidation Coatings Formed at Different Voltages on the In Situ Growth of Layered Double Hydroxides and Their Corrosion Protection. Journal of the Electrochemical Society, 2018, 165, C317-C327.	1.3	56
120	Thermal desorption spectrometer for measuring ppm concentrations of trapped hydrogen. International Journal of Hydrogen Energy, 2018, 43, 7600-7617.	3.8	29
121	Corrosion of Ti35Zr28Nb in Hanks' solution and 3.5 wt% NaCl solution. Materials and Corrosion - Werkstoffe Und Korrosion, 2018, 69, 197-206.	0.8	12
122	The influence of two common sterilization techniques on the corrosion of Mg and its alloys for biomedical applications. Journal of Biomedical Materials Research - Part B Applied Biomaterials, 2018, 106, 1907-1917.	1.6	16
123	Equivalent Hydrogen Fugacity during Electrochemical Charging of 980DP Steel Determined by Thermal Desorption Spectroscopy. Advanced Engineering Materials, 2018, 20, 1700469.	1.6	21
124	Hydrogen Trapping in Some Automotive Martensitic Advanced High‣trength Steels. Advanced Engineering Materials, 2018, 20, 1700468.	1.6	46
125	The Influence of Hydrogen on the Low Cycle Fatigue Behavior of Medium Strength 3.5NiCrMoV Steel Studied Using Notched Specimens. Advanced Engineering Materials, 2018, 20, 1700680.	1.6	6
126	Enhanced Corrosion Resistance of Anodic Films Containing Alumina Nanoparticles on as-rolled AZ31 alloy. International Journal of Electrochemical Science, 2018, 13, 7157-7174.	0.5	7

#	Article	IF	CITATIONS
127	Stress corrosion cracking of EV31A in 0.1â€ <sup>−</sup> M Na2SO4 saturated with Mg(OH)2. Journal of Magnesium and Alloys, 2018, 6, 337-345.	5.5	12
128	Viewpoint - Understanding Mg corrosion in the body for biodegradable medical implants. Scripta Materialia, 2018, 154, 92-100.	2.6	156
129	The influence of microstructure on the hydrogen embrittlement susceptibility of martensitic advanced high strength steels. Materials Today Communications, 2018, 17, 1-14.	0.9	72
130	Electrochemical and Mechanical Aspects of Hydrogen Embrittlement Evaluation of Martensitic Steels. , 2018, , 201-225.		4
131	Influence of Hydrogen on Steel Components for Clean Energy. Corrosion and Materials Degradation, 2018, 1, 3-26.	1.0	27
132	Evaluation of automobile service performance using laboratory testing. Materials Science and Technology, 2018, 34, 1893-1909.	0.8	13
133	Active corrosion protection by a smart coating based on a MgAl-layered double hydroxide on a cerium-modified plasma electrolytic oxidation coating on Mg alloy AZ31. Corrosion Science, 2018, 139, 370-382.	3.0	271
134	Influence of pH on the growth behaviour of Mg–Al LDH films. Surface Engineering, 2018, 34, 674-681.	1.1	39
135	Understanding the Corrosion of Mg and Mg Alloys. , 2018, , 515-534.		27
136	Evaluation of the influence of hydrogen on some commercial DP, Q&P and TWIP advanced high-strength steels during automobile service. Engineering Failure Analysis, 2018, 94, 249-273.	1.8	24
137	Deformation mechanism and microstructure evolution during on-line heating rolling of AZ31B Mg thin sheets. Materials Characterization, 2017, 124, 266-275.	1.9	11
138	Hydrogen influence on some advanced high-strength steels. Corrosion Science, 2017, 125, 114-138.	3.0	90
139	Communication—Fabrication of Protective Layered Double Hydroxide Films by Conversion of Anodic Films on Magnesium Alloy. Journal of the Electrochemical Society, 2017, 164, C339-C341.	1.3	39
140	Corrosion of the galvanizing of galvanizedâ€steel electricity transmission towers. Materials and Corrosion - Werkstoffe Und Korrosion, 2017, 68, 902-910.	0.8	10
141	Combined influence of Be and Ca on improving the high-temperature oxidation resistance of the magnesium alloy Mg-9Al-1Zn. Corrosion Science, 2017, 122, 1-11.	3.0	42
142	Equivalent hydrogen fugacity during electrochemical charging of some martensitic advanced high-strength steels. Corrosion Science, 2017, 127, 45-58.	3.0	44
143	Influence of crystallographic texture and grain size on the corrosion behaviour of as-extruded Mg alloy AZ31 sheets. Corrosion Science, 2017, 126, 374-380.	3.0	158
144	Effect of thermal-mechanical processing on microstructure and mechanical properties of duplex-phase Mg-8Li-3Al-0.4Y alloy. Transactions of Nonferrous Metals Society of China, 2017, 27, 2587-2597.	1.7	16

#	Article	IF	CITATIONS
145	Influence of hydrogen on the mechanical and fracture properties of some martensitic advanced high strength steels in simulated service conditions. Corrosion Science, 2016, 111, 602-624.	3.0	65
146	An Hydrogen Evolution Method for the Estimation of the Corrosion Rate of Magnesium Alloys. , 2016, , 565-572.		29
147	Influence of surface condition on the corrosion of ultra-high-purity Mg alloy wire. Corrosion Science, 2016, 108, 66-75.	3.0	36
148	Influence of high pressure during solidification on the microstructure and strength of Mg-Zn-Y alloys. Journal of Rare Earths, 2016, 34, 435-440.	2.5	15
149	A review on hot tearing of magnesium alloys. Journal of Magnesium and Alloys, 2016, 4, 151-172.	5.5	104
150	Hydrogen Concentration in Dualâ€Phase (DP) and Quenched and Partitioned (Q&P) Advanced High‧trength Steels (AHSS) under Simulated Service Conditions Compared with Cathodic Charging Conditions. Advanced Engineering Materials, 2016, 18, 1588-1599.	1.6	28
151	Influence of Ag micro-alloying on the thermal stability and ageing characteristics of a Cu–14Fe in-situ composite. Materials Science & Engineering A: Structural Materials: Properties, Microstructure and Processing, 2016, 673, 1-7.	2.6	38
152	Hydrogen trapping in some advanced high strength steels. Corrosion Science, 2016, 111, 770-785.	3.0	105
153	A review of the influence of hydrogen on the mechanical properties of DP, TRIP, and TWIP advanced high-strength steels for auto construction. Corrosion Reviews, 2016, 34, 127-152.	1.0	70
154	Solidification of Mg-Zn-Y Alloys at 6ÂGPa Pressure: Nanostructure, Phases Formed, and Their Stability. Journal of Materials Engineering and Performance, 2016, 25, 3830-3837.	1.2	1
155	Corrosion and passivation of magnesium alloys. Corrosion Science, 2016, 111, 835-845.	3.0	300
156	A review of hydrogen embrittlement of martensitic advanced high-strength steels. Corrosion Reviews, 2016, 34, 153-186.	1.0	141
157	Oxidation of magnesium alloys at elevated temperatures in air: A review. Corrosion Science, 2016, 112, 734-759.	3.0	141
158	Effect of H 3 BO 3 on corrosion in 0.01 M NaCl solution of the interface between low alloy steel A508 and alloy 52 M. Corrosion Science, 2016, 102, 469-483.	3.0	22
159	Oxidation resistance of Mg–9Al–1Zn alloys micro-alloyed with Be. Scripta Materialia, 2016, 115, 38-41.	2.6	38
160	Electrochemical Dealloying of a Ternary Al67Cu18Sn15 Alloy Compared with that of a Binary Al75Cu25 Alloy. ECS Transactions, 2015, 66, 23-30.	0.3	0
161	Stress corrosion cracking of high-strength AZ31 processed by high-ratio differential speed rolling. Journal of Magnesium and Alloys, 2015, 3, 271-282.	5.5	22
162	Effect of Heat Treatment on the Microstructure and Properties of Deformation-Processed Cu-7Cr In Situ Composites. Journal of Materials Engineering and Performance, 2015, 24, 4340-4345.	1.2	17

ANDREJ ATRENS

#	Article	IF	CITATIONS
163	CFD Convective Flow Simulation of the Varying Properties of CO2-H2O Mixtures in Geothermal Systems. Scientific World Journal, The, 2015, 2015, 1-8.	0.8	2
164	Stress corrosion cracking of several solution heat-treated Mg–X alloys. Corrosion Science, 2015, 96, 121-132.	3.0	41
165	Stress corrosion cracking of several hot-rolled binary Mg–X alloys. Corrosion Science, 2015, 98, 6-19.	3.0	26
166	Concurrence of de-alloying and re-alloying in a ternary Al <sub>67</sub> Cu <sub>18</sub> Sn <sub>15</sub> alloy and the fabrication of 3D nanoporous Cu–Sn composite structures. RSC Advances, 2015, 5, 9574-9580.	1.7	7
167	Influence of casting porosity on the corrosion behaviour of Mg0.1Si. Corrosion Science, 2015, 94, 255-269.	3.0	37
168	Corrosion and stress corrosion cracking of ultra-high-purity Mg5Zn. Corrosion Science, 2015, 93, 330-335.	3.0	36
169	Review of Recent Developments in the Field of Magnesium Corrosion. Advanced Engineering Materials, 2015, 17, 400-453.	1.6	595
170	Revolutionising biodegradable biomaterials – significance ofÂmagnesium and its alloys. , 2015, , 3-28.		2
171	Reversible hydrogen trapping in a 3.5NiCrMoV medium strength steel. Corrosion Science, 2015, 96, 112-120.	3.0	83
172	Optimisation of the high velocity oxygen fuel (HVOF) parameters to produce effective corrosion control coatings on AZ91 magnesium alloy. Materials and Corrosion - Werkstoffe Und Korrosion, 2015, 66, 423-433.	0.8	32
173	Creation of bimodal porous copper materials by an annealing-electrochemical dealloying approach. Electrochimica Acta, 2015, 164, 288-296.	2.6	49
174	Corrosion of Mg for biomedical applications. , 2015, , 81-102.		1
175	The influence of hydrogen on the mechanical and fracture properties of some martensitic advanced high strength steels studied using the linearly increasing stress test. Corrosion Science, 2015, 99, 98-117.	3.0	115
176	The influence of pH on the corrosion rate of high-purity Mg, AZ91 and ZE41 in bicarbonate buffered Hanks' solution. Corrosion Science, 2015, 101, 182-192.	3.0	114
177	Strain rate dependence in the nanoindentation-induced deformation of Mg-Al intermetallic compounds produced by packed powder diffusion coating. Metals and Materials International, 2015, 21, 793-798.	1.8	3
178	Possible dissolution pathways participating in the Mg corrosion reaction. Corrosion Science, 2015, 92, 173-181.	3.0	56
179	Influence of hot rolling on the corrosion behavior of several Mg–X alloys. Corrosion Science, 2015, 90, 176-191.	3.0	140
180	Evaluation of Coatings for Mg Alloys for Biomedical Applications. Advanced Engineering Materials, 2015, 17, 58-67.	1.6	18

11

#	Article	lF	CITATIONS
181	Water condensation in carbon-dioxide-based engineered geothermal power generation. Geothermics, 2014, 51, 397-405.	1.5	6
182	Nanomechanical properties of Mg–Al intermetallic compounds produced by packed powder diffusion coating (PPDC) on the surface of AZ91E. Journal of Alloys and Compounds, 2014, 587, 527-532.	2.8	27
183	Influence of the chloride ion concentration on the corrosion of high-purity Mg, ZE41 and AZ91 in buffered Hank's solution. Journal of Materials Science: Materials in Medicine, 2014, 25, 329-345.	1.7	49
184	Low apparent valence of Mg during corrosion. Corrosion Science, 2014, 88, 434-443.	3.0	62
185	Determination of the hydrogen fugacity during electrolytic charging of steel. Corrosion Science, 2014, 87, 239-258.	3.0	106
186	Influence of hydrogen on the mechanical properties of some medium-strength Ni–Cr–Mo steels. Materials Science & Engineering A: Structural Materials: Properties, Microstructure and Processing, 2014, 617, 200-210.	2.6	33
187	Corrosion behaviour of laser surface melted magnesium alloy AZ91D. Materials & Design, 2014, 57, 40-50.	5.1	73
188	Influence of experimental parameters on thermal desorption spectroscopy measurements during evaluation of hydrogen trapping. Journal of Nuclear Materials, 2014, 450, 32-41.	1.3	34
189	Corrosion performance and mechanical properties of sputter-deposited MgY and MgGd alloys. Corrosion Science, 2014, 78, 43-54.	3.0	55
190	Galvanostatic anodic polarisation of WE43. Journal of Magnesium and Alloys, 2014, 2, 197-202.	5.5	17
191	Influence of a high magnetic field on the microstructure and properties of a Cu–Fe–Ag in situ composite. Materials Science & Engineering A: Structural Materials: Properties, Microstructure and Processing, 2013, 584, 114-120.	2.6	46
192	Thermal desorption spectroscopy study of the interaction of hydrogen with TiC precipitates. Metals and Materials International, 2013, 19, 741-748.	1.8	60
193	Corrosion of ultra-high-purity Mg in 3.5% NaCl solution saturated with Mg(OH)2. Corrosion Science, 2013, 75, 78-99.	3.0	271
194	A critical review of the influence of hydrogen on the mechanical properties of medium-strength steels. Corrosion Reviews, 2013, 31, 85-103.	1.0	93
195	Comments on the paper entitled "Observations of the galvanostatic dissolution of pure magnesium― by N.T. Kirkland, G. Williams and N. Birbilis. Corrosion Science, 2013, 77, 403-406.	3.0	9
196	Corrosion behaviour in salt spray and in 3.5% NaCl solution saturated with Mg(OH)2 of as-cast and solution heat-treated binary Mg–RE alloys: RE=Ce, La, Nd, Y, Gd. Corrosion Science, 2013, 76, 98-118.	3.0	143
197	A Framework for Fast Graph-Based Pattern Matching in Conceptual Models. , 2013, , .		1
198	Corrosion behaviour in salt spray and in 3.5% NaCl solution saturated with Mg(OH)2 of as-cast and solution heat-treated binary Mg–X alloys: X=Mn, Sn, Ca, Zn, Al, Zr, Si, Sr. Corrosion Science, 2013, 76, 60-97.	3.0	212

#	Article	IF	CITATIONS
199	Advances in Mg corrosion and research suggestions. Journal of Magnesium and Alloys, 2013, 1, 177-200.	5.5	397
200	Stress corrosion cracking of high-strength steels. Corrosion Reviews, 2013, 31, 1-31.	1.0	74
201	The influence of hydrogen on 3.5NiCrMoV steel studied using the linearly increasing stress test. Corrosion Science, 2013, 67, 193-203.	3.0	49
202	Microstructure and Properties of a Deformation-Processed Cu-Cr-Ag In Situ Composite by Directional Solidification. Journal of Materials Engineering and Performance, 2013, 22, 3723-3727.	1.2	13
203	The in vivo and in vitro corrosion of high-purity magnesium and magnesium alloys WZ21 and AZ91. Corrosion Science, 2013, 75, 354-366.	3.0	174
204	Neutron residual stress measurements in rails. Neutron News, 2013, 24, 9-13.	0.1	9
205	Thermal desorption spectroscopy study of experimental Ti/S containing steels. Materials Science and Technology, 2013, 29, 261-267.	0.8	15
206	A Novel Heat Treatment for Excavator Dipper Teeth Manufactured from Lowâ€Carbon Lowâ€Alloy Steel. Steel Research International, 2013, 84, 89-93.	1.0	2
207	Overview of the Mg Corrosion Mechanism. ECS Transactions, 2013, 50, 335-344.	0.3	8
208	Evaluation from First Principles the Structural Stability of Mg Containing Different Amounts of Al Atoms under High Pressure. Applied Mechanics and Materials, 2013, 391, 56-60.	0.2	1
209	Production of High Purity Mg-X Rare Earth Binary Alloys Using Zr. Materials Science Forum, 2013, 765, 301-305.	0.3	2
210	Mechanics of modern test methods and quantitative-accelerated testing for hydrogen embrittlement. , 2012, , 237-273.		6
211	The ignition temperature of Mg alloys WE43, AZ31 and AZ91. Corrosion Science, 2012, 54, 139-142.	3.0	77
212	Influence of Al and Y on the ignition and flammability of Mg alloys. Corrosion Science, 2012, 55, 153-163.	3.0	68
213	Galvanostatic anodic polarisation curves and galvanic corrosion of high purity Mg in 3.5% NaCl saturated with Mg(OH)2. Corrosion Science, 2012, 60, 296-308.	3.0	92
214	Corrosion behaviour of a nominally high purity Mg ingot produced by permanent mould direct chill casting. Corrosion Science, 2012, 61, 185-207.	3.0	158
215	Galvanostatic Anodic Polarization Curves and Galvanic Corrosion of AZ31B in 0.01 <scp>M</scp> Na <sub>2</sub> SO <sub>4</sub> Saturated with Mg(OH) <sub>2</sub> . Advanced Engineering Materials, 2012, 14, 324-334.	1.6	31
216	Production of High Purity Magnesium Alloys by Melt Purification with Zr. Advanced Engineering Materials, 2012, 14, 477-490.	1.6	56

ANDREJ ATRENS

#	Article	IF	CITATIONS
217	Flammability of Mg–X Binary Alloys. Advanced Engineering Materials, 2012, 14, 772-784.	1.6	41
218	Plug-In Specimens for Measurement of the Corrosion Rate of Mg Alloys. Jom, 2012, 64, 657-663.	0.9	9
219	Surface damage on new AS60 rail caused by wheel slip. Engineering Failure Analysis, 2012, 22, 152-165.	1.8	50
220	Role of second phase cementite and martensite particles on strength and strain hardening in a plain C-Mn steel. Materials Science & Engineering A: Structural Materials: Properties, Microstructure and Processing, 2012, 549, 222-227.	2.6	18
221	An innovative specimen configuration for the study of Mg corrosion. Corrosion Science, 2011, 53, 226-246.	3.0	368
222	Corrosion of high purity Mg, AZ91, ZE41 and Mg2Zn0.2Mn in Hank's solution at room temperature. Corrosion Science, 2011, 53, 862-872.	3.0	136
223	Influence of the applied stress rate on the stress corrosion cracking of 4340 and 3.5NiCrMoV steels under conditions of cathodic hydrogen charging. Corrosion Science, 2011, 53, 2419-2429.	3.0	47
224	Corrosion of high purity Mg, Mg2Zn0.2Mn, ZE41 and AZ91 in Hank's solution at 37 °C. Corrosion Science, 2011, 53, 3542-3556.	3.0	191
225	Barriers to Pediatric Pain Management: A Nursing Perspective. Pain Management Nursing, 2011, 12, 154-162.	0.4	64
226	Strength and toughness tradeoffs for an ultrafine-grain size ferrite/cementite steel produced by warm-rolling and annealing. Materials Science & Engineering A: Structural Materials: Properties, Microstructure and Processing, 2011, 528, 8157-8168.	2.6	20
227	Corrosion mechanism applicable to biodegradable magnesium implants. Materials Science and Engineering B: Solid-State Materials for Advanced Technology, 2011, 176, 1609-1636.	1.7	355
228	The ductile to brittle transition for C–Mn steel with an ultrafine grain ferrite/cementite microstructure. Materials Science & Engineering A: Structural Materials: Properties, Microstructure and Processing, 2011, 528, 7228-7237.	2.6	8
229	Stress Corrosion Cracking of Magnesium Alloys. Advanced Engineering Materials, 2011, 13, 11-18.	1.6	54
230	Identification of the effective grain size responsible for the ductile to brittle transition temperature for steel with an ultrafine grain size ferrite/cementite microstructure with a bimodal ferrite grain size distribution. Materials Science & amp; Engineering A: Structural Materials: Properties, Microstructure and Processing, 2011, 528, 4217-4221.	2.6	14
231	Stress corrosion cracking (SCC) of magnesium alloys. , 2011, , 341-380.		11
232	Stress corrosion cracking (SCC) of magnesium (Mg) alloys. , 2011, , 299-364.		7
233	Testing and evaluation methods for stress corrosion cracking (SCC) in metals. , 2011, , 133-166.		4
234	Corrosion of magnesium (Mg) alloys and metallurgical influence. , 2011, , 117-165.		25

#	Article	IF	CITATIONS
235	Numerical modelling of galvanic corrosion of magnesium (Mg) alloys. , 2011, , 455-483.		6
236	Environmentally Assisted Cracking of Magnesium Alloys. Materials Science Forum, 2011, 690, 373-376.	0.3	0
237	Electricity generation using a carbon-dioxide thermosiphon. Geothermics, 2010, 39, 161-169.	1.5	109
238	Effect of Ag micro-alloying on the microstructure and properties of Cu–14Fe in situ composite. Materials Science & Engineering A: Structural Materials: Properties, Microstructure and Processing, 2010, 527, 4953-4958.	2.6	39
239	Influence of microstructure on tensile properties and fatigue crack growth in extruded magnesium alloy AM60. International Journal of Fatigue, 2010, 32, 411-419.	2.8	52
240	Influence of Si on glass forming ability and properties of the bulk amorphous alloy Mg60Cu30Y10. Materials Science & Engineering A: Structural Materials: Properties, Microstructure and Processing, 2010, 527, 7475-7479.	2.6	4
241	Influence of Ag micro-alloying on the microstructure and properties of Cu–7Cr in situ composite. Journal of Alloys and Compounds, 2010, 500, L22-L25.	2.8	24
242	Electrochemical reactivity, surface composition and corrosion mechanisms of the complex metallic alloy Al3Mg2. Corrosion Science, 2010, 52, 562-578.	3.0	78
243	Measurement of the corrosion rate of magnesium alloys using Tafel extrapolation. Corrosion Science, 2010, 52, 579-588.	3.0	774
244	The influence of applied stress rate on the stress corrosion cracking of 4340 and 3.5NiCrMoV steels in distilled water at 30°C. Corrosion Science, 2010, 52, 1042-1051.	3.0	51
245	The influence of yttrium (Y) on the corrosion of Mg–Y binary alloys. Corrosion Science, 2010, 52, 3687-3701.	3.0	299
246	Stress Corrosion Cracking. , 2010, , 864-901.		9
247	Influence of heat treatment and microstructure on the corrosion of magnesium alloy Mg-10Gd-3Y-0.4Zr. Journal of Applied Electrochemistry, 2009, 39, 913-920.	1.5	62
248	Hydrogen embrittlement and rock bolt stress corrosion cracking. Engineering Failure Analysis, 2009, 16, 164-175.	1.8	77
249	Composition and morphology of the film formed on a lead alloy under conditions typical of the electro-winning of copper. Hydrometallurgy, 2009, 96, 14-26.	1.8	17
250	CO <sub>2</sub> Thermosiphon for Competitive Geothermal Power Generation. Energy & Fuels, 2009, 23, 553-557.	2.5	95
251	Calculated phase diagrams and the corrosion of die-cast Mg–Al alloys. Corrosion Science, 2009, 51, 602-619.	3.0	296
252	A first quantitative XPS study of the surface films formed, by exposure to water, on Mg and on the Mg–Al intermetallics: Al3Mg2 and Mg17Al12. Corrosion Science, 2009, 51, 1115-1127.	3.0	234

#	Article	IF	CITATIONS
253	An exploratory study of the corrosion of Mg alloys during interrupted salt spray testing. Corrosion Science, 2009, 51, 1277-1292.	3.0	238
254	ToF-SIMS depth profile of the surface film on pure magnesium formed by immersion in pure water and the identification of magnesium hydride. Corrosion Science, 2009, 51, 1883-1886.	3.0	66
255	Corrosion protection of AZ91 magnesium alloy by anodizing in niobium and zirconium-containing electrolytes. Corrosion Science, 2009, 51, 3030-3038.	3.0	103
256	Comparison of the corrosion behaviour in 5% NaCl solution of Mg alloys NZ30K and AZ91D. Journal of Applied Electrochemistry, 2008, 38, 207-214.	1.5	56
257	Influence of cobalt ions on the anodic oxidation of a lead alloy under conditions typical of copper electrowinning. Journal of Applied Electrochemistry, 2008, 38, 215-224.	1.5	9
258	Electrochemical behavior of magnesium alloys AZ91D, AZCe2, and AZLa1 in chloride and sulfate solutions. Journal of Applied Electrochemistry, 2008, 38, 251-257.	1.5	39
259	Influence of lead dioxide surface films on anodic oxidation of a lead alloy under conditions typical of copper electrowinning. Journal of Applied Electrochemistry, 2008, 38, 569-577.	1.5	14
260	Calculated phase diagrams, iron tolerance limits, and corrosion of Mg-Al alloys. Jom, 2008, 60, 39-44.	0.9	78
261	Fractography of Stress Corrosion Cracking of Mg-Al Alloys. Metallurgical and Materials Transactions A: Physical Metallurgy and Materials Science, 2008, 39, 1157-1173.	1.1	62
262	Influence of Microstructure on Corrosion of Asâ€cast ZE41. Advanced Engineering Materials, 2008, 10, 104-111.	1.6	130
263	Stress Corrosion Cracking (SCC) in Mgâ€Al Alloys Studied using Compact Specimens. Advanced Engineering Materials, 2008, 10, 453-458.	1.6	31
264	Corrosion of AZ91 in 1N NaCl and the Mechanism of Magnesium Corrosion. Advanced Engineering Materials, 2008, 10, 583-587.	1.6	42
265	Effect of applied stress and microstructure on sulfide stress cracking resistance of pipeline steels subject to hydrogen sulfide. Materials Science & Engineering A: Structural Materials: Properties, Microstructure and Processing, 2008, 478, 43-47.	2.6	46
266	Metallurgical aspects of rock bolt stress corrosion cracking. Materials Science & Engineering A: Structural Materials: Properties, Microstructure and Processing, 2008, 491, 8-18.	2.6	37
267	Six Sigma review of root causes of corrosion incidents in hot potassium carbonate acid gas removal plant. Engineering Failure Analysis, 2008, 15, 480-496.	1.8	16
268	SCC of commercial steels exposed to high hydrogen fugacity. Engineering Failure Analysis, 2008, 15, 617-641.	1.8	44
269	Comparison of the linearly increasing stress test and the constant extension rate test in the evaluation of transgranular stress corrosion cracking of magnesium. Materials Science & Engineering A: Structural Materials: Properties, Microstructure and Processing, 2008, 472, 97-106.	2.6	106
270	Characterisation of stress corrosion cracking (SCC) of Mg–Al alloys. Materials Science & Engineering A: Structural Materials: Properties, Microstructure and Processing, 2008, 488, 339-351.	2.6	150

#	Article	IF	CITATIONS
271	The effect of crystallographic orientation on the active corrosion of pure magnesium. Scripta Materialia, 2008, 58, 421-424.	2.6	253
272	Influence of the β-phase morphology on the corrosion of the Mg alloy AZ91. Corrosion Science, 2008, 50, 1939-1953.	3.0	524
273	Influence of pH and chloride ion concentration on the corrosion of Mg alloy ZE41. Corrosion Science, 2008, 50, 3168-3178.	3.0	378
274	Stress corrosion cracking of rare-earth containing magnesium alloys ZE41, QE22 and Elektron 21 (EV31A) compared with AZ80. Materials Science & Engineering A: Structural Materials: Properties, Microstructure and Processing, 2008, 480, 529-539.	2.6	155
275	Influence of Homogenization Annealing of AZ91 on Mechanical Properties and Corrosion Behavior. Advanced Engineering Materials, 2008, 10, 93-103.	1.6	78
276	Experimental Measurement and Computer Simulation of Galvanic Corrosion of Magnesium Coupled to Steel. Advanced Engineering Materials, 2007, 9, 65-74.	1.6	82
277	Recent Insights into the Mechanism of Magnesium Corrosion and Research Suggestions. Advanced Engineering Materials, 2007, 9, 177-183.	1.6	263
278	The Negative Difference Effect and Unipositive Mg+. Advanced Engineering Materials, 2007, 9, 292-297.	1.6	162
279	Evaluation of the delayed hydride cracking mechanism for transgranular stress corrosion cracking of magnesium alloys. Materials Science & Engineering A: Structural Materials: Properties, Microstructure and Processing, 2007, 466, 18-31.	2.6	87
280	Relationship between yield strength and grain size for a bimodal structural ultrafine-grained ferrite/cementite steel. Scripta Materialia, 2007, 57, 857-860.	2.6	79
281	Influence of solution chemistry and surface condition on the critical inhibitor concentration for solutions typical of hot potassium carbonate CO2 removal plant. Journal of Materials Science, 2007, 42, 7762-7771.	1.7	8
282	Passivity breakdown of carbon steel in hot potassium carbonate solutions. Journal of Materials Science, 2007, 42, 9940-9946.	1.7	5
283	Stress corrosion cracking in magnesium alloys: Characterization and prevention. Jom, 2007, 59, 49-53.	0.9	39
284	An evaluation of steels subjected to rock bolt SCC conditions. Engineering Failure Analysis, 2007, 14, 1351-1393.	1.8	34
285	Atom probe field ion microscope measurements of carbon segregation at an α:α grain boundary and service failures by intergranular stress corrosion cracking. Corrosion Science, 2006, 48, 79-92.	3.0	31
286	Influence of anodising current on the corrosion resistance of anodised AZ91D magnesium alloy. Corrosion Science, 2006, 48, 1939-1959.	3.0	141
287	Influence of geometry on galvanic corrosion of AZ91D coupled to steel. Corrosion Science, 2006, 48, 2133-2153.	3.0	139
288	Atmospheric corrosion of copper and the colour, structure and composition of natural patinas on copper. Corrosion Science, 2006, 48, 2480-2509.	3.0	152

#	Article	IF	CITATIONS
289	The corrosion performance of anodised magnesium alloys. Corrosion Science, 2006, 48, 3531-3546.	3.0	111
290	Corrosion resistance of anodised single-phase Mg alloys. Surface and Coatings Technology, 2006, 201, 492-503.	2.2	91
291	Stress Corrosion Cracking and Hydrogen Diffusion in Magnesium. Advanced Engineering Materials, 2006, 8, 749-751.	1.6	69
292	Corrosion Behaviour of the Microstructural Constituents of AZ Alloys. , 2006, , 423-431.		1
293	Characterisation of TG-SCC In Pure Magnesium and AZ91 Alloy. , 2006, , 979-980.		0
294	Understanding the Corrosion Mechanism: A Framework for Improving the Performance of Magnesium Alloys. , 2005, , 507-516.		3
295	A Critical Review of the Stress Corrosion Cracking (SCC) of Magnesium Alloys. Advanced Engineering Materials, 2005, 7, 659-693.	1.6	386
296	Boundary element method predictions of the influence of the electrolyte on the galvanic corrosion of AZ91D coupled to steel. Materials and Corrosion - Werkstoffe Und Korrosion, 2005, 56, 259-270.	0.8	46
297	Simulation of galvanic corrosion of magnesium coupled to a steel fastener in NaCl solution. Materials and Corrosion - Werkstoffe Und Korrosion, 2005, 56, 468-474.	0.8	106
298	A study on stress corrosion cracking and hydrogen embrittlement of AZ31 magnesium alloy. Materials Science & Engineering A: Structural Materials: Properties, Microstructure and Processing, 2005, 399, 308-317.	2.6	126
299	Material influence on the stress corrosion cracking of rock bolts. Engineering Failure Analysis, 2005, 12, 201-235.	1.8	49
300	Influence of the β phase on the corrosion performance of anodised coatings on magnesium–aluminium alloys. Corrosion Science, 2005, 47, 2760-2777.	3.0	130
301	Research Directions in Magnesium Corrosion Arising from the Wolfsburg Conference. Advanced Engineering Materials, 2004, 6, 83-84.	1.6	12
302	Evaluation of the BEASY program using linear and piecewise linear approaches for the boundary conditions. Materials and Corrosion - Werkstoffe Und Korrosion, 2004, 55, 845-852.	0.8	52
303	Analysis of service stress corrosion cracking in a natural gas transmission pipeline, active or dormant?. Engineering Failure Analysis, 2004, 11, 3-18.	1.8	30
304	Stress corrosion cracking and hydrogen embrittlement of an Al–Zn–Mg–Cu alloy. Acta Materialia, 2004, 52, 4727-4743.	3.8	220
305	Stress corrosion cracking fracture mechanisms in rock bolts. Journal of Materials Science, 2003, 38, 3813-3829.	1.7	43
306	Review of stress corrosion cracking of pipeline steels in "low―and "high―pH solutions. Journal of Materials Science, 2003, 38, 127-132.	1.7	165

#	Article	IF	CITATIONS
307	Microstructure and grain boundary microanalysis of X70 pipeline steel. Journal of Materials Science, 2003, 38, 323-330.	1.7	21
308	Comparative atmospheric corrosion of primary and cold rolled copper in Australia. Journal of Materials Science, 2003, 38, 995-1005.	1.7	11
309	Analysis of mixing distribution in an engine-like configuration. International Journal of Energy Research, 2003, 27, 1039-1050.	2.2	1
310	Understanding Magnesium Corrosion—A Framework for Improved Alloy Performance. Advanced Engineering Materials, 2003, 5, 837-858.	1.6	1,744
311	Environmental influence on the stress corrosion cracking of rock bolts. Engineering Failure Analysis, 2003, 10, 521-558.	1.8	92
312	SCC initiation for X65 pipeline steel in the "high―pH carbonate/bicarbonate solution. Corrosion Science, 2003, 45, 2199-2217.	3.0	99
313	Strategic maintenance management. Journal of Quality in Maintenance Engineering, 2002, 8, 287-305.	1.0	165
314	Precipitation hardening of Cu-Fe-Cr alloys part I Mechanical and electrical properties. Journal of Materials Science, 2001, 36, 2711-2719.	1.7	74
315	Cu-rich corner of the Cu-Fe-Cr phase diagram. Journal of Materials Science Letters, 2001, 20, 2213-2215.	0.5	8
316	Quaternary Cu-0.7%Cr-0.3%Fe-X alloys. Journal of Materials Science, 2001, 36, 4763-4777.	1.7	7
317	Precipitation hardening of Cu-Fe-Cr alloys part II Microstructural characterisation. Journal of Materials Science, 2001, 36, 2721-2741.	1.7	26
318	Cold worked Cu-Fe-Cr alloys. Journal of Materials Science, 2001, 36, 5497-5510.	1.7	33
319	Implications of specimen preparation and of surface contamination for the measurement of the grain boundary carbon concentration of steels using x-ray microanalysis in an UHV FESTEM. Surface and Interface Analysis, 2000, 29, 23-32.	0.8	31
320	Boundary characterisation of X65 pipeline steel using analytical electron microscopy. Journal of Materials Science, 1999, 34, 1711-1719.	1.7	22
321	Microstructure of X52 and X65 pipeline steels. Journal of Materials Science, 1999, 34, 1721-1728.	1.7	44
322	The crack tip strain field of AISI 4340 Part I Measurement technique. Journal of Materials Science, 1999, 34, 4909-4920.	1.7	13
323	The crack tip strain field of AISI 4340 Part III Hydrogen influence. Journal of Materials Science, 1999, 34, 4931-4936.	1.7	21
324	The crack tip strain field of AISI 4340 Part II Experimental measurements. Journal of Materials Science, 1999, 34, 4921-4929.	1.7	6

#	Article	IF	CITATIONS
325	Corrosion Mechanisms of Magnesium Alloys. Advanced Engineering Materials, 1999, 1, 11-33.	1.6	1,977
326	Corrosion Mechanisms of Magnesium Alloys. Advanced Engineering Materials, 1999, 1, 11-33.	1.6	29
327	Linearly-increasing-stress testing of carbon steel in 4 N NaNO3 and in Bayer liquor. Journal of Materials Science, 1998, 33, 783-788.	1.7	23
328	ESEM observations of SCC initiation for 4340 high strength steel in distilled water. Journal of Materials Science, 1998, 33, 405-415.	1.7	26
329	Stress corrosion crack propagation in AerMet 100. Journal of Materials Science, 1998, 33, 775-781.	1.7	49
330	Measurement of grain boundary composition for X52 pipeline steel. Acta Materialia, 1998, 46, 5677-5687.	3.8	39
331	Corrosion behaviour of AZ21, AZ501 and AZ91 in sodium chloride. Corrosion Science, 1998, 40, 1769-1791.	3.0	750
332	The chemistry of copper patination. Corrosion Science, 1998, 40, 2029-2050.	3.0	86
333	Influence of microstructure on the corrosion of diecast AZ91D. Corrosion Science, 1998, 41, 249-273.	3.0	838
334	The Secondary Passive Film for Type 304 Stainless Steel in 0.5 M  H 2 SO 4. Journal of the Elec Society, 1997, 144, 3697-3704.	trochemic 1.3	al 40
335	SCC INITIATION FOR 4340 IN DISTILLED WATER. , 1997, , 375-382.		1
336	The electrochemical corrosion of pure magnesium in 1 N NaCl. Corrosion Science, 1997, 39, 855-875.	3.0	541
337	The anodic dissolution of magnesium in chloride and sulphate solutions. Corrosion Science, 1997, 39, 1981-2004.	3.0	767
338	Atmospheric corrosion of copper at Heron Island. Materials Letters, 1997, 30, 141-146.	1.3	11
339	Properties of rapidly solidified binary copper alloys. Materials Letters, 1997, 31, 87-92.	1.3	17
340	Environmental assisted fracture for 4340 steel in water and air of various humidities. Journal of Materials Science, 1997, 32, 6519-6523.	1.7	23
341	The initiation and propagation of stress corrosion cracking in AISI 4340 and 3.5 Niî—,Crî—,Moî—,V rotor steel in constant load tests. Corrosion Science, 1996, 38, 1159-1169.	3.0	43
342	Initiation of stress corrosion cracking for pipeline steels in a carbonate-bicarbonate solution. Metallurgical and Materials Transactions A: Physical Metallurgy and Materials Science, 1996, 27, 2686-2691.	1.1	65

#	Article	IF	CITATIONS
343	Influence of environmental variables on erosion-corrosion of carbon steel in spent liquor reheaters in Bayer plant. Wear, 1995, 189, 107-116.	1.5	5
344	A new impinging jet test rig used to identify the important parameters in service erosion-corrosion in bayer liquor and to study the damage morphology. Wear, 1994, 176, 163-171.	1.5	9
345	Estimation of the unknown parameters in the melt-spinning process. Journal of Materials Science, 1994, 29, 544-547.	1.7	2
346	The thermokinetic modeling of substrate rapid solidification. Jom, 1994, 46, 48-50.	0.9	2
347	Room temperature creep of high strength steels. Acta Metallurgica Et Materialia, 1994, 42, 1493-1508.	1.9	68
348	Analytical electron microscopy of grain boundaries in high-strength steels. Acta Metallurgica Et Materialia, 1994, 42, 1139-1146.	1.9	14
349	Relevance of free-surface temperature to thermal and kinetic factors in melt spinning. Journal of Materials Science, 1993, 28, 4003-4009.	1.7	1
350	A TEM study on the microstructure of rapidly solidified Cu-Y alloys. Journal of Materials Science, 1993, 28, 6809-6814.	1.7	3
351	The stress corrosion cracking of as-quenched 4340 and 3.5NiCrMoV steels under stress rate control in distilled water at 90ŰC. Corrosion Science, 1993, 34, 1385-1402.	3.0	55
352	A new metastable orthorhombic phase Cu9Y. Acta Metallurgica Et Materialia, 1993, 41, 2877-2885.	1.9	11
353	A TEM study on the microstructure of rapidly solidified Cuî—,Co alloys. Acta Metallurgica Et Materialia, 1993, 41, 563-568.	1.9	11
354	Linearly increasing stress test (LIST) for SCC research. Measurement Science and Technology, 1993, 4, 1281-1292.	1.4	96
355	SCC of copper using the linearly increasing stress test. Scripta Metallurgica Et Materialia, 1992, 26, 1447-1450.	1.0	21
356	ESCA studies of Cr-Co alloys. Applied Physics A: Solids and Surfaces, 1992, 54, 270-278.	1.4	25
357	ESCA studies of Ni-Cr alloys. Applied Physics A: Solids and Surfaces, 1992, 54, 343-349.	1.4	30
358	ESCA studies of Fe-Ti alloys. Applied Physics A: Solids and Surfaces, 1992, 54, 500-507.	1.4	23
359	Rapid solidification characteristics in melt spinning. Materials Science & Engineering A: Structural Materials: Properties, Microstructure and Processing, 1992, 159, 243-251.	2.6	16
360	ESCA studies of Si-Fe alloys. Applied Physics A: Solids and Surfaces, 1991, 53, 273-281.	1.4	32

#	Article	IF	CITATIONS
361	Grain Boundary Electrochemistry and the Stress Corrosion Cracking of High Strength Steels. Materials Science Forum, 1991, 44-45, 139-152.	0.3	7
362	Accelerated Atmospheric Corrosion Of Copper And Copper Alloys. Corrosion Engineering Science and Technology, 1990, 25, 271-278.	0.3	14
363	Passive films on stainless steels in aqueous media. Applied Physics A: Solids and Surfaces, 1990, 50, 287-300.	1.4	53
364	ESCA studies of nitrogen-containing stainless steels. Applied Physics A: Solids and Surfaces, 1990, 51, 411-418.	1.4	86
365	The role of crack tip strain rate in the stress corrosion cracking of high strength steels in water. Metallurgical and Materials Transactions A - Physical Metallurgy and Materials Science, 1989, 20, 889-895.	1.4	41
366	Nature of oxygen in the passive film on stainless steels in 0.1 M NaCl solution. Applied Physics A: Solids and Surfaces, 1989, 48, 385-389.	1.4	3
367	ESCA-studies of the surface film formed on stainless steels by exposure to 0.1 M NaCl solution at various controlled potentials. Applied Physics A: Materials Science and Processing, 1988, 46, 51-65.	1.1	20
368	ESCA-Studies of the structure and composition of the passive film formed on stainless steels by various immersion temperatures in 0.1 M NaCl solution. Applied Physics A: Solids and Surfaces, 1988, 45, 83-91.	1.4	15
369	Discussion of "a new method for the simulation of electron diffraction patterns: The algorithm and its application to previous studiesâ€: Scripta Metallurgica, 1988, 22, 1695-1699.	1.2	4
370	Microstructure of as-quenched 3.5 NiCrMoV rotor steel — Part II. Double diffraction. Materialwissenschaft Und Werkstofftechnik, 1987, 18, 179-185.	0.5	20
371	ESCA-studies of the structure and composition of the passive film formed on stainless steels by various immersion times in 0.1 M NaCl solution. Applied Physics A: Solids and Surfaces, 1987, 42, 149-165.	1.4	111
372	Microstructure of as-quenched 3.5NiCrMoV rotor steel. Part I. General structure and retained austenite. Materialwissenschaft Und Werkstofftechnik, 1987, 18, 165-170.	0.5	15
373	Microstructure of as-quenched 3.5 NiCrMoV rotor steel. Part III. Carbide Precipitation. Materialwissenschaft Und Werkstofftechnik, 1987, 18, 344-353.	0.5	8
374	Stress corrosion cracking and hydrogen embrittlement of cold worked AISI type 304 austenitic stainless steel in mode I and mode III. Materials Science and Technology, 1986, 2, 1066-1073.	0.8	13
375	Stress corrosion cracking and hydrogen embrittlement of cold worked AISI type 304 austenitic stainless steel in mode I and mode III. Materials Science and Technology, 1986, 2, 1066-1073.	0.8	1
376	Corrosion of stainless steels in chloride solution: An XPS investigation of passive films. Applied Physics A: Solids and Surfaces, 1985, 38, 1-18.	1.4	88
377	Corrosion Potential oscillations. Materialwissenschaft Und Werkstofftechnik, 1984, 15, 309-314.	0.5	6
378	Stress-corrosion-cracking of Zircaloy-4 cladding tubes. Journal of Nuclear Materials, 1984, 126, 91-102.	1.3	12

#	Article	IF	CITATIONS
379	Stress-corrosion-cracking of Zircaloy-4 cladding tubes. Journal of Nuclear Materials, 1984, 126, 103-110.	1.3	4
380	Reply to comments on "Calculation of intrinsic damping and modulus defect― Scripta Metallurgica, 1983, 17, 257-260.	1.2	0
381	Subsurface crack initiation in high cycle fatigue in Ti6A14V and in a typical martensitic stainless steel. Scripta Metallurgica, 1983, 17, 601-606.	1.2	95
382	Environmental Conditions Leading to Pitting/Crevice Corrosion of a Typical 12% Chromium Stainless Steel at 80 C. Corrosion, 1983, 39, 483-487.	0.5	20
383	CORROSION POTENTIAL OSCILLATIONS OF STAINLESS STEELS IN AQUEOUS CHLORIDE SOLUTIONS. , 1983, , 631-636.		3
384	Initiation of fatigue cracks in duplex stainless steel X4 CrMnNiMoN2664 in 4N NaCl at 80°C, pH=2 and 7. Metals Technology, 1982, 9, 117-121.	0.3	4
385	DISLOCATION RELAXATION IN A RANDOM ARRAY OF SOLUTES. Journal De Physique Colloque, 1981, 42, C5-319-C5-324.	0.2	1
386	A metallographic study of the terminal solubility of hydrogen in zirconium at low hydrogen concentrations. Journal of Nuclear Materials, 1980, 88, 42-50.	1.3	53
387	Electrochemical studies of hydrogen diffusion and permeability in Ni. Corrosion Science, 1980, 20, 673-684.	3.0	75
388	Dislocation damping and hydrogen pinning in austenitic stainless steels. Journal of Applied Physics, 1977, 48, 4247-4251.	1.1	24
389	Calculation of intrinsic damping and modulus defect. Scripta Metallurgica, 1977, 11, 497-498.	1.2	4
390	Further comments on â€~amplitude-dependent damping in zirconium'. Scripta Metallurgica, 1977, 11, 107-108.	1.2	60
391	The diffusion of oxygen in alpha-zirconium. Journal of Nuclear Materials, 1977, 67, 254-264.	1.3	115
392	Estimation of the number of pinning points per network length from an analysis of an amplitude dependent damping peak. Scripta Metallurgica, 1976, 10, 1089-1093.	1.2	3
393	Comment on analysis of the amplitude dependent damping data in terms of the Granato-Lücke model. Scripta Metallurgica, 1976, 10, 211-214.	1.2	1
394	Anelastic relaxation and the diffusion of oxygen in alpha-zirconium. Journal of Nuclear Materials, 1976, 62, 1-8.	1.3	16
395	Effect of praseodymium on the internal friction in a zirconium-oxygen single crystal. Journal of Nuclear Materials, 1976, 62, 121-122.	1.3	2
396	Strain-amplitude-dependent internal friction in annealed zirconium-oxygen alloys. Journal of Nuclear Materials, 1975, 55, 267-272.	1.3	3

#	Article	IF	CITATIONS
397	Comments on amplitude dependent damping in zirconium. Scripta Metallurgica, 1975, 9, 1313-1316.	1.2	4
398	Dependence of the pinning point dislocation interaction energy on the dislocation structure in zirconium oxygen alloys. Scripta Metallurgica, 1974, 8, 401-412.	1.2	27
399	A Preliminary Quantitative XPS Study of the Surface Films Formed on Pure Magnesium and on Magnesium-Aluminium Intermetallics by Exposure to High-Purity Water. Materials Science Forum, 0, 618-619, 255-262.	0.3	5
400	Corrosion of AZ91 - Influence of the $\hat{I}^2$ -Phase Morphology. Materials Science Forum, 0, 618-619, 473-478.	0.3	14
401	Magnesium Corrosion in Different Solutions. Materials Science Forum, 0, 690, 369-372.	0.3	5
402	An Innovative Specimen for Mg Corrosion Studies. Materials Science Forum, 0, 690, 365-368.	0.3	4
403	Microstructure and Electrical Resistivity of In Situ Cu-Fe Microcomposites. Journal of Materials Engineering and Performance, 0, , 1.	1.2	1